



0-3

**Preparation of 0-3 Polymer-based Piezoelectric Composites
with $(\text{Pb}_{1-x}, \text{Bi}_x)(\text{Ti}_{1-y}, \text{Fe}_y)\text{O}_3$ Powders**

本 論 文 金 敬 泰 工 學 碩 士 學 位 論 文 認 准

인

인

인

2001 2

1.	1
2.	3
2.1	3
2.2	5
2.2.1	-	5
2.2.2	8
2.3	11
3.	13
3.1	(Pb _{1-x} , Bi _x)(Ti _{1-y} , Fe _y)O ₃ powder	13
3.2	(Pb _{1-x} , Bi _x)(Ti _{1-y} , Fe _y)O ₃ /polymer	17
3.3	Hysteresis loop	20
4.	22
4.1	(Pb _{1-x} , Bi _x)(Ti _{1-y} , Fe _y)O ₃ powder	22
4.2	(Pb _{0.5} , Bi _{0.5})(Ti _{0.5} , Fe _{0.5})O ₃ /polymer	27
5.	37
	39

Fig. 2.1. Applications of piezoelectric composites.

Fig. 2.2. Connectivity patterns for a diphasic solid. Each phase has zero-, one-, two-, or three-dimensional connectivity to itself. In the 3-1 composite, for instance, the shaded phase is three-dimensionally connected. Arrows are used to indicate the connected directions.

Fig. 2.3. Schematic representation of piezoelectric composites with 0-3, 1-3, and 3-3 connectivity.

Fig. 2.4. The composites consisted of dielectric continuous medium and piezoelectric ellipsoidal particles.

Fig. 3.1. Flow diagram for piezoelectric ceramic preparation.

Fig. 3.2. Sintering condition of piezoelectric ceramics.

Fig. 3.3. Ni plating process.

Fig. 4.1. XRD patterns of the powders treated at various temperatures.

Fig. 4.2. XRD patterns of $(\text{Pb}_{1-x}\text{Bi}_x)(\text{Ti}_{1-y}\text{Fe}_y)\text{O}_3$ powder ($x=y$).

Fig. 4.3. XRD patterns of $(\text{Pb}_{1-x}\text{Bi}_x)(\text{Ti}_{1-y}\text{Fe}_y)\text{O}_3$ powder ($x \neq y$).

Fig. 4.4. XRD patterns of each heat-treatment conditions.

- (a) 900 °C, Pb-atmosphere (b) 900 °C, air-atmosphere
(c) 1000 °C, Pb-atmosphere (d) 1000 °C, air-atmosphere

Fig. 4.5. SEM micrographs of (a) ceramic powder sintered at 900 °C and (b) 1000 °C, and composite with (c) UP RF1001, (d) KBR1729, (e) Bakelite powder, and (f) Transoptic powder.

Fig. 4.6. Dielectric properties of each specimens. (1kHz)

Fig. 4.7. Hysteresis loop of specimens : composite with Bakelite powder and $(\text{Pb}_{0.5}\text{Bi}_{0.5})(\text{Ti}_{10.5}\text{Fe}_{0.5})\text{O}_3$ calcined at (a) 900 °C, and (b) 1000 °C.

Fig. 4.8. Remanent polarizations of the 50vol% of $(\text{Pb}_{0.5}\text{Bi}_{0.5})(\text{Ti}_{10.5}\text{Fe}_{0.5})\text{O}_3$ calcined at 900 °C composite with each voltage.

Fig. 4.9. Remanent polarizations of the composites with Bakelite powder with each vol% of $(\text{Pb}_{0.5}\text{Bi}_{0.5})(\text{Ti}_{10.5}\text{Fe}_{0.5})\text{O}_3$.

Table. 3.1. Composition of each $(\text{Pb}_{1-x}\text{Bi}_x)(\text{Ti}_{1-y}\text{Fe}_y)\text{O}_3$ powder.

Table. 3.2. Polymers used in the present study.

Table. 4.1. Tetragonality of each specimen.

**Preparation of 0-3 Polymer-based Piezoelectric Composites
with $(\text{Pb}_{1-x}, \text{Bi}_x)(\text{Ti}_{1-y}, \text{Fe}_y)\text{O}_3$ Powders**

Kyung-Tae Kim

Dept. of Materials Engineering
Graduate School
Korea Maritime University

ABSTRACT

Piezoelectric materials are used extensively in many transducer applications. However they have limited utility in transducers used under hydrostatic conditions because of their low hydrostatic piezoelectric coefficient(d_h) have also limited utility in ultrasonic field due to small voltage coefficient(g_{33}) and large acoustic impedance.

To improve the magnitude of hydrostatic piezoelectric coefficient and voltage coefficient, the composite of piezoelectric materials and polymer with different patterns have been prepared. In addition, these composites having lower acoustic impedance and smaller dielectric constant than those of solid piezoelectric materials, make it easier to obtain good impedance matching with water of the human body.

Because of these advantages, piezoelectric composites would be used in many fields such as measuring instruments, diagnostic ultrasonic transducer, information processing instruments and acoustic devices.

Especially, these composites have advantage of making a shape using ceramic powder that cannot produce by sintering.

In this study, we produced the composites using $(\text{Pb}_{1-x}, \text{Bi}_x)(\text{Ti}_{1-y}, \text{Fe}_y)\text{O}_3$ powder which cannot produce by sintering because of its high

tetragonality that create high inner stress. $(\text{Pb}_{1-x}, \text{Bi}_x)(\text{Ti}_{1-y}, \text{Fe}_y)\text{O}_3$ /Epoxy 0-3 piezoelectric composites were prepared for investigating the effects of volume fraction of $(\text{Pb}_{1-x}, \text{Bi}_x)(\text{Ti}_{1-y}, \text{Fe}_y)\text{O}_3$ on the dielectric, piezoelectric properties of composites. $(\text{Pb}_{1-x}\text{Bi}_x)(\text{Ti}_{1-y}\text{Fe}_y)\text{O}_3$ powder, which has high tetragonality and voltage coefficient (g_{33}) was prepared from oxide mixture of PbO , Bi_2O_3 , TiO_2 and Fe_2O_3 . Then, $(\text{Pb}_{1-x}, \text{Bi}_x)(\text{Ti}_{1-y}, \text{Fe}_y)\text{O}_3$ particles were mixed with epoxy, piezoelectrically inactive species. After poling, dielectric, and piezoelectric properties were investigated.

1.

1940 BaTiO₃ , PZT
가
(hydrophone),
(actuator), sonar
가
가 , 가 polymer
가
1973 Pauer가 PZT
Kyiatama, Banno 가
^{15),16)} 가
1978 Newnham
10가
가
가 가
0-3
0-3
가
0-3 , Pb(Zr,Ti)O₃ PbTiO₃
(matrix phase) polyurethane,
silicon rubber, chloroprene rubber, eccogel, polyvinyliden fluoride
가

가 .

tetragonality (c/a) . 가

$(Pb_{1-x}, Bi_x)(Ti_{1-y}, Fe_y)O_3$ polymer .

PbO, Bi_2O_3 , TiO_2 , Fe_2O_3 $(Pb_{1-x}, Bi_x)(Ti_{1-y}, Fe_y)O_3$ (x,y=0.2-0.8)

Bi- Pb

가 Bi 가

가 tetragonality .

가 tetragonality .

polymer 0-3

2.

2.1

(polarization) (electric field) 가
(deformation) ^{1),2)} 가
1880 Curie가 가
rochelle salt, KH_2PO_4 , $(\text{NH}_4)\text{H}_2\text{PO}_4$ 가 ³⁾ 가
. 1945 , perovskite
 BaTiO_3 1000 가
. BaTiO_3 , 1947
Roberts BaTiO_3 가 가
, 가
Mason 가
. BaTiO_3 curie point가
^{2),3)} perovskite PbTiO_3 ,
 CaTiO_3 , PbZrO_3 가
 $\text{Pb}(\text{Zr,Ti})\text{O}_3$,
(K)가 60% Curie 400
filter, buzzer, speaker, transformer, resonator,
sonar, cleaner, ignitor ^{1),2),4)}
3 32
20 가
, 가
가 ¹⁾
(T), (E), (S),

(D) 가

$$d = \left(\frac{D}{T}\right)_E = \left(\frac{S}{E}\right)_T$$

$$e = \left(\frac{D}{S}\right)_E = - \left(\frac{T}{E}\right)_E$$

$$g = \left(\frac{E}{T}\right)_D = \left(\frac{S}{D}\right)_T$$

$$h = - \left(\frac{E}{S}\right)_D = - \left(\frac{T}{D}\right)_S$$

가

$$S = s^E T + d {}_1E$$

$$D = dT + \varepsilon^T E$$

$$T = c^E T - e {}_1E$$

$$D = \varepsilon S + \varepsilon^S E$$

$$S = s^D T + g {}_1D$$

$$E = - gT + \beta^T D$$

$$T = c^D T - h {}_1D$$

$$E = - hS + \beta^S D$$

s elastic compliance, c elastic stiffness, ,

1)

2.2

가 . 가 가

2.2.1 -

(40kHz) hydrophone

가 thermister

가 ^{5),6)}

가 brittle ,

sheet / 가 .

, bulk /

가 .

[]

- (10 μ m) 가 .

- , .

- .(10mHz GHz)

- 가 .(.)

- 가 .

- .
- 가 .

[]

- 가 30 80 (100 가)

- 가 .
(Quartz, PZT) 가 DC 가 .

, 가 ,
sheet array
(動壓) 가 ,
(, printer roll ,
) 가 .¹⁾

hot press key board가 .

, ,
. Fig. 2.1 .¹⁾

, electomechanical transducer ink jets,

, 가 , ,

polymer , SiC-polymer package substrate, superconductor-polymer PTC-

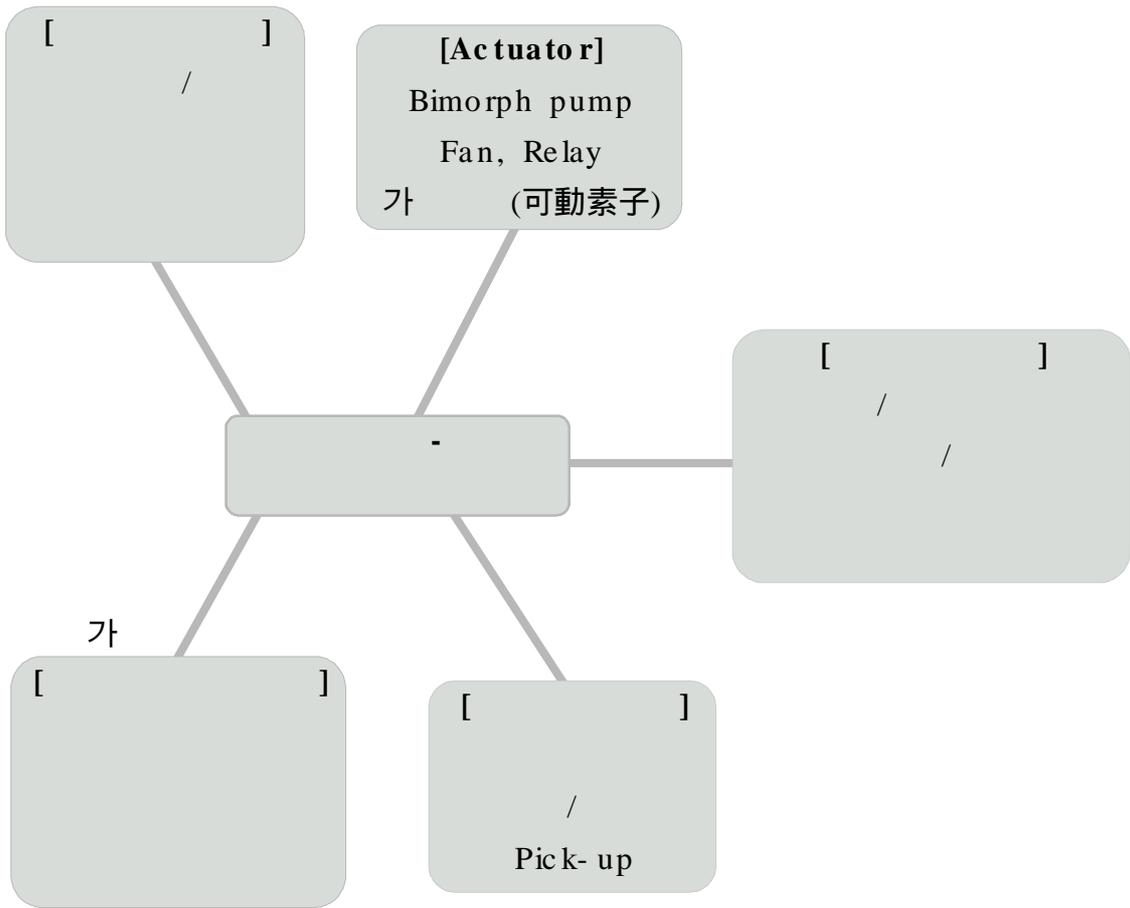


Fig. 2.1. Applications of piezoelectric composites.(ref. 1)

2.2.2

1978 Newnham (piezoelectric active phase)
(nonpiezoelectric phase)
, (connectivity) 10가
Fig. 2.2 (phase)
가 , (connectivity)
.
, .
3-3, 1-3, 0-3 가
^{1),2),3),4)}
3-3 3
Skinner, Rittenmyer . lost wax
plastic spheres . 3-3 가
, , impedance matching
^{1),4)}
1-3 1 Harrison
PZT powder 가
. PZT rod
spurrs epoxy
. 1-3
가
^{7),8)}
0-3 .
가 가 가
, , 가 .
3-0, 3-1, 3-2, 2-2

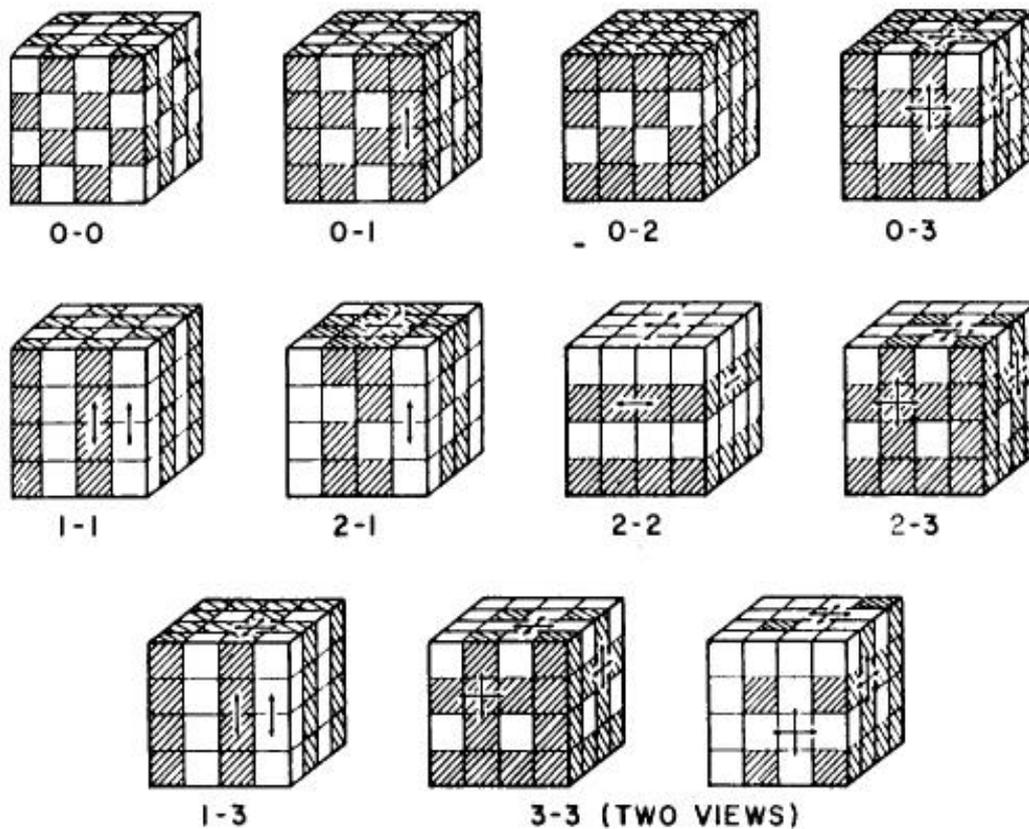


Fig. 2.2. Connectivity patterns for a diphasic solid. Each phase has zero-, one-, two-, or three-dimensional connectivity to itself. In the 3-1 composite, for instance, the shaded phase is three-dimensional connected. Arrows are used to indicate the connected directions.(ref. 1)

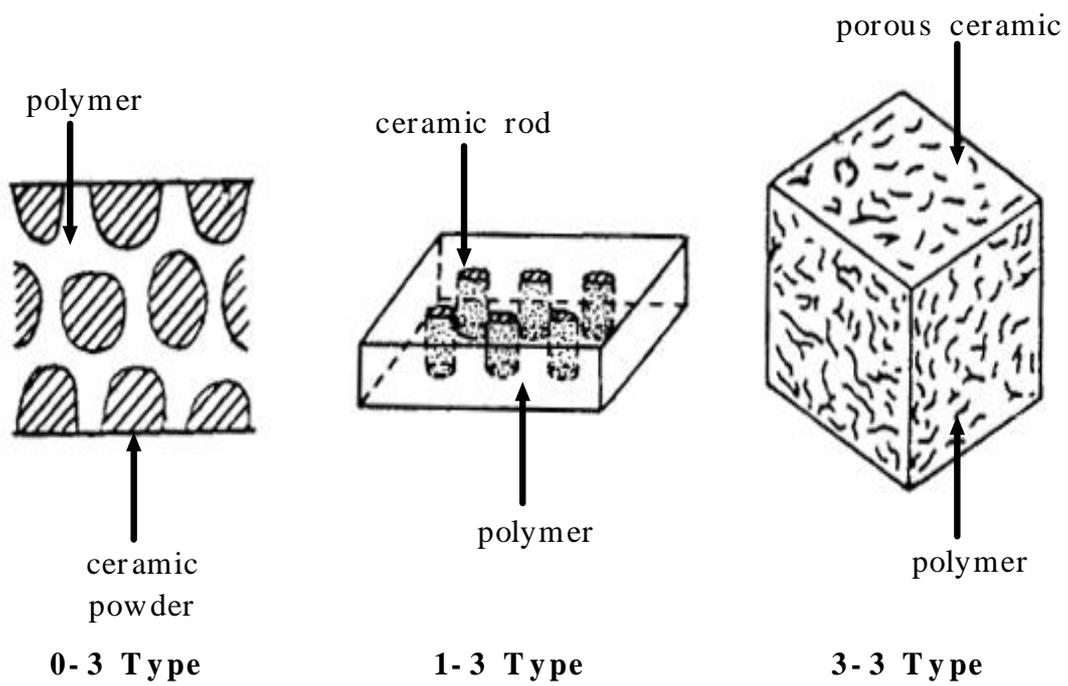


Fig. 2.3. Schematic representation of piezoelectric composites with 0-3, 1-3, and 3-3 connectivity.

가 . Fig. 2.3.

가 0-3, 1-3, 3-3

2.3

0-3 , matrix 가
 , 2 가
 . matrix dispersoid 가
 , dispersoid 가
 (matrix) (dispersoid)
 - 2 2 가
 . T.Yamada

0-3

^{9),10),11)}

Fig. 2.4.

matrix

, Maxwell

$$K = K_1 \left\{ 1 + \frac{nq(K_2 - K_1)}{nK_1 + (K_2 - K_1)(1 - q)} \right\}$$

, K_1 matrix , K_2 dispersoid
 , q dispersoid , n dispersoid (

3 가) .

가 ,

(K_2)가 matrix (K_1) 가

, 가

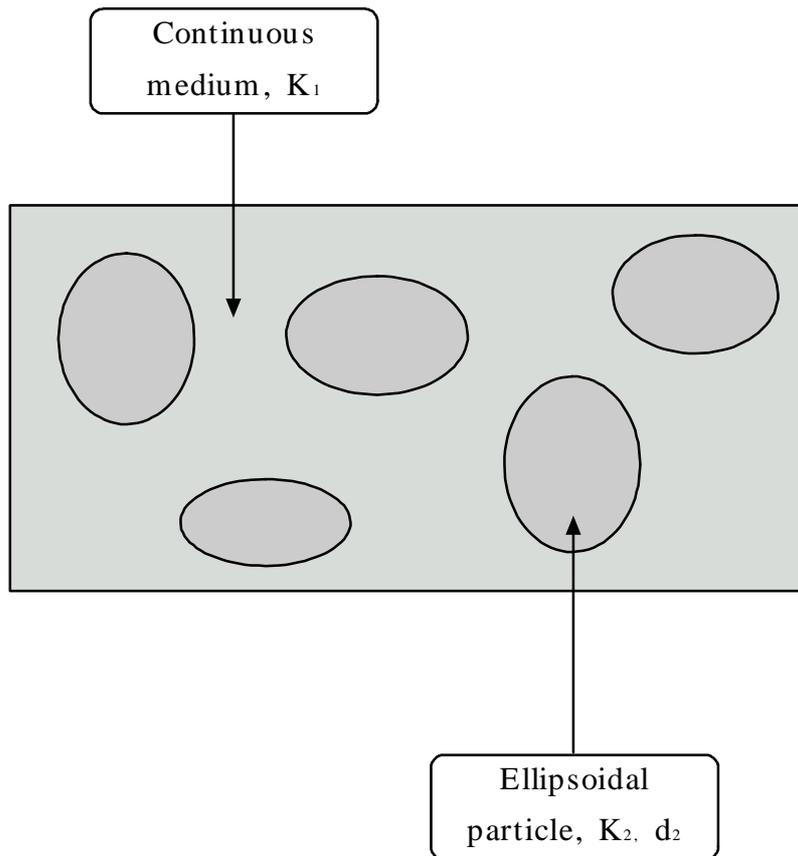


Fig. 2.4 The composites consisted of dielectric continuous medium and piezoelectric ellipsoidal particles.

3.

3.1 $(\text{Pb}_{1-x}, \text{Bi}_x)(\text{Ti}_{1-y}, \text{Fe}_y)\text{O}_3$ powder

, MOD
 가
 ,
 $(\text{Pb}_{1-x}, \text{Bi}_x)(\text{Ti}_{1-y}, \text{Fe}_y)\text{O}_3$
 .
 $(\text{Pb}_{1-x}, \text{Bi}_x)(\text{Ti}_{1-y}, \text{Fe}_y)\text{O}_3$ Bi-
 Pb
 가 Bi 가 Bi
 가 가 가
 . tetragonality .
^{10),12),13),14),15)}
 PbO, Bi₂O₃, TiO₂ Fe₂O₃ x y 0.2, 0.3,
 0.4, 0.5, 0.8
 . Table 3.1 .
 , 가 ,
 , 700 2
 .
 15mm
 1.13ton/cm² 가 disc .
 Fig. 3.1 .
 Pb- Pb

Table. 3.1. Composition of each $(\text{Pb}_{1-x}\text{Bi}_x)(\text{Ti}_{1-y}\text{Fe}_y)\text{O}_3$ powder.

x	y				
		PbO	Bi ₂ O ₃	TiO ₂	Fe ₂ O ₃
0.2	0.2	4.64	1.17	1.6	0.4
	0.5	4.64	1.17	1	1
	0.8	4.64	1.17	0.4	1.6
0.3	0.3	2.906	1.294	1	0.444
0.4	0.4	2.933	1.944	1	0.666
0.5	0.2	2.96	2.92	1.6	0.4
	0.5	2.96	2.92	1	1
	0.8	2.96	2.92	0.4	1.6
0.8	0.2	1.29	4.67	1.6	0.4
	0.5	1.29	4.67	1	1
	0.8	1.29	4.67	0.4	1.6

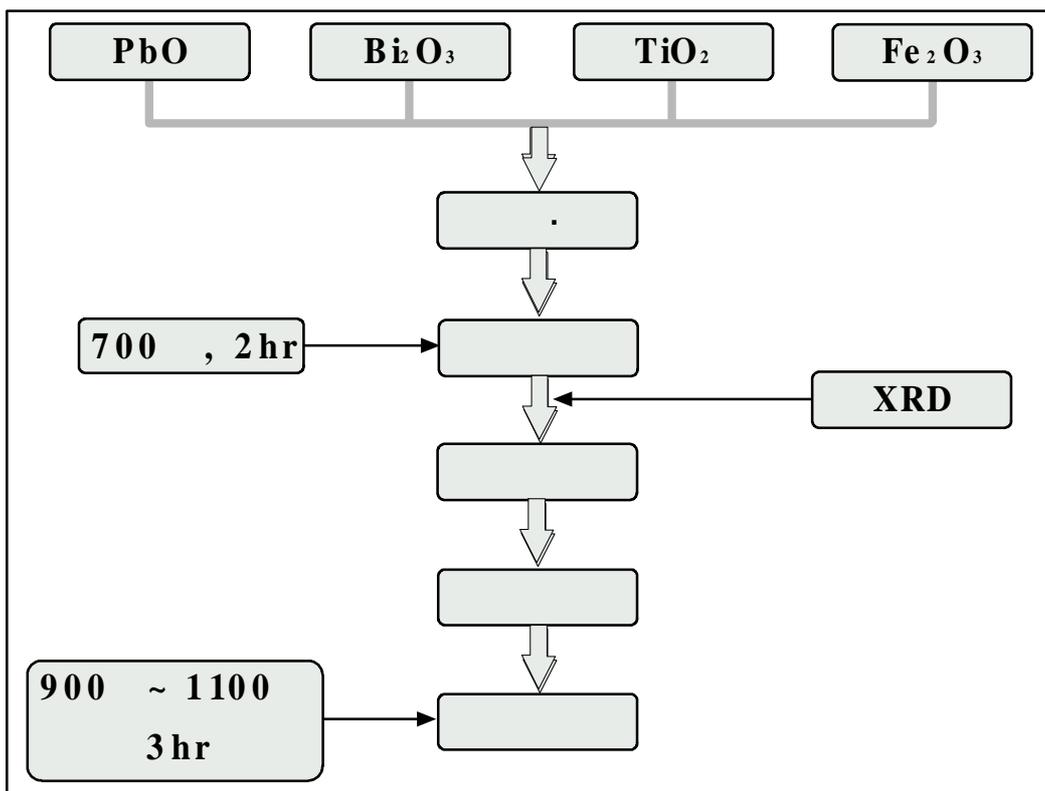


Fig. 3.1. Flow diagram for piezoelectric ceramic preparation.

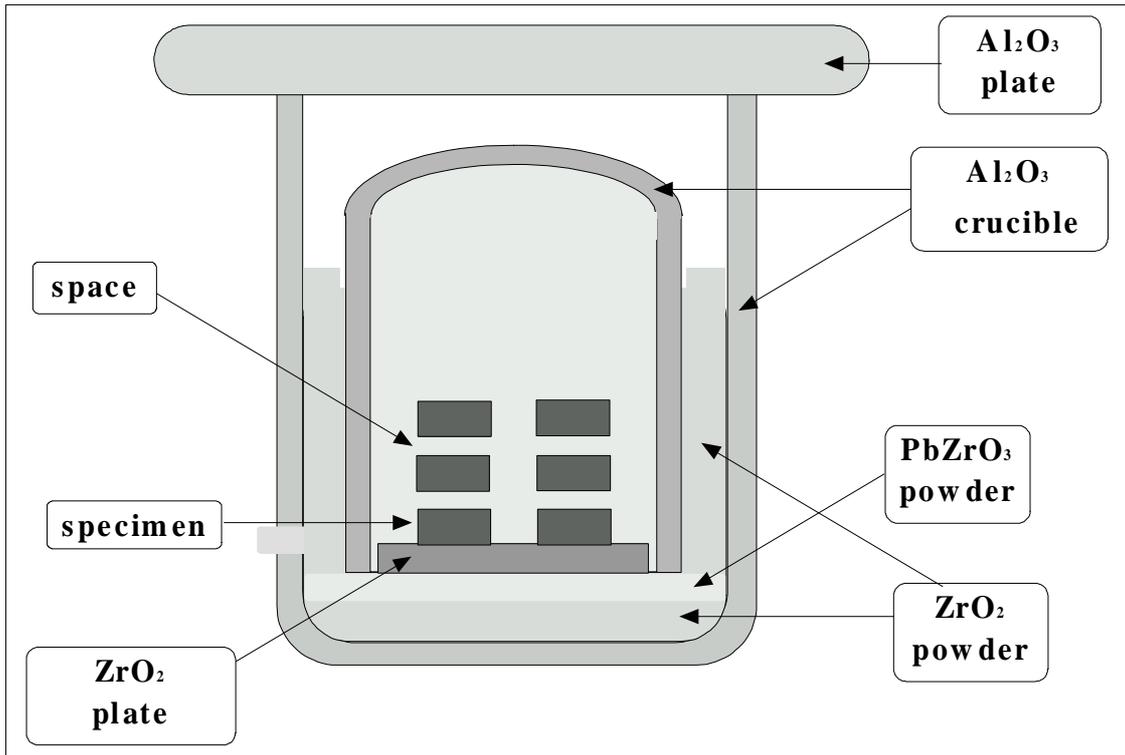


Fig. 3.2. Sintering condition of piezoelectric ceramics.

Fig. 3.2. ZrO_2 Plate
 PbZrO_3 Pb 가
 가 ZrO_2
 Pb 가
 XRD
 가 $(\text{Pb}_{1-x}, \text{Bi}_x)(\text{Ti}_{1-y}, \text{Fe}_y)\text{O}_3$

3.2 $(\text{Pb}_{1-x}, \text{Bi}_x)(\text{Ti}_{1-y}, \text{Fe}_y)\text{O}_3$ /polymer

$(\text{Pb}_{1-x}, \text{Bi}_x)(\text{Ti}_{1-y}, \text{Fe}_y)\text{O}_3$ tetragonality
 가 $(\text{Pb}_{1-x}, \text{Bi}_x)(\text{Ti}_{1-y}, \text{Fe}_y)\text{O}_3$
 polymer 0-3 $(\text{Pb}_{1-x}, \text{Bi}_x)(\text{Ti}_{1-y}, \text{Fe}_y)\text{O}_3$
 $\text{Fe}_y)\text{O}_3$ polymer
 0-3 가
 가 , 가
 0-3 $(\text{Pb}_{1-x}, \text{Bi}_x)(\text{Ti}_{1-y}, \text{Fe}_y)\text{O}_3$ Fig. 3.2.
 Pb-
 XRD
 Bi-
 $(\text{Pb}_{1-x}, \text{Bi}_x)(\text{Ti}_{1-y}, \text{Fe}_y)\text{O}_3$
 $(\text{Pb}_{1-x}, \text{Bi}_x)(\text{Ti}_{1-y}, \text{Fe}_y)\text{O}_3$ 가

Table. 3.2. Polymers used in the present study.

Polyester resin		Hardening condition	Density (g/cm³)	Composite density (%)
Solid	Black Bakelite Powder	130~ 180 20~ 30 kN 10~ 20 min	1.4	95~ 98%
	Transoptic Powder		1.42	
Liquid	UP RF100 1	R T, 8hr	1.38	70~ 80%
	KBR1729	120 , 2hr	1.2	

3.3

Hysteresis loop

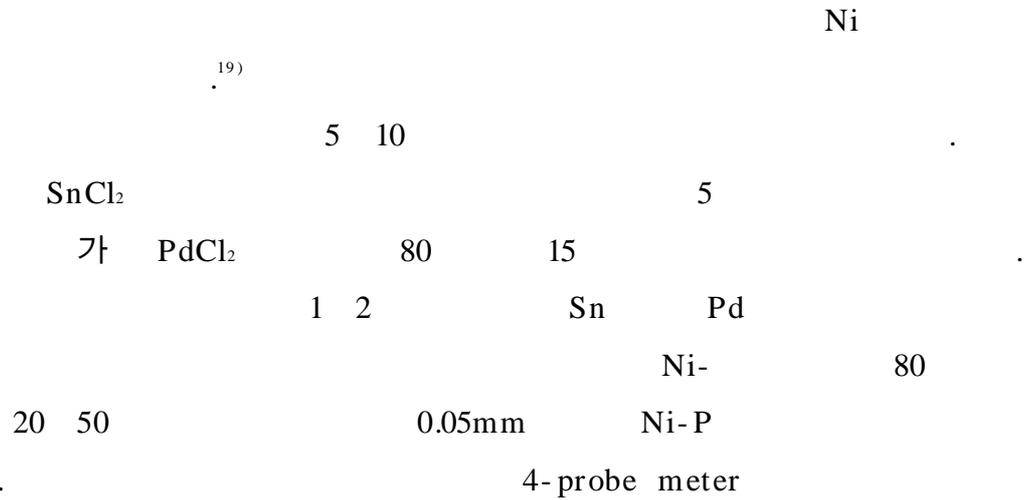
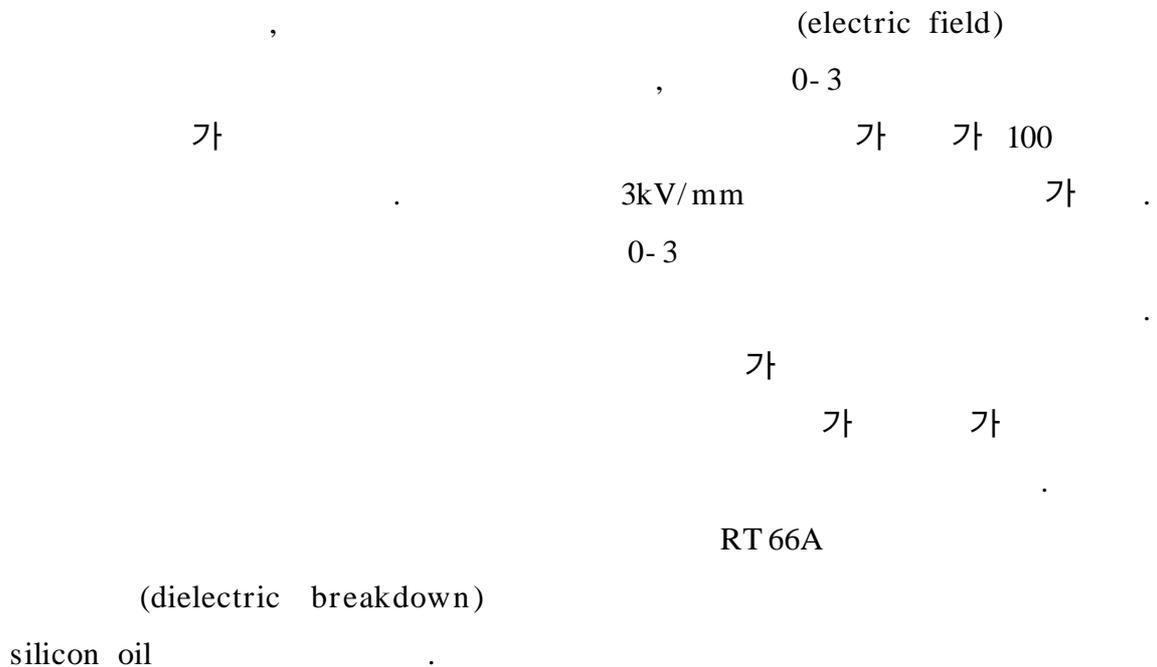


Fig. 3.3



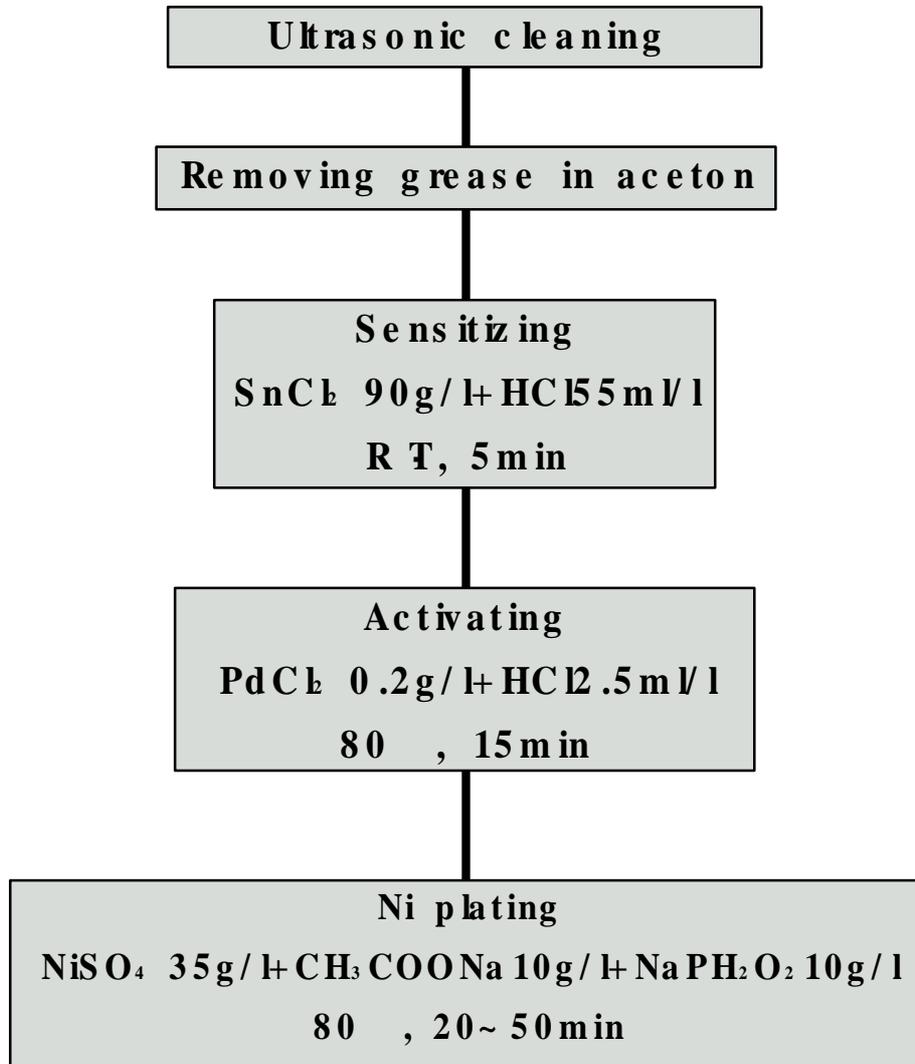


Fig. 3.3. Ni plating process.

4.

4.1 $(\text{Pb}_{1-x}, \text{Bi}_x)(\text{Ti}_{1-y}, \text{Fe}_y)\text{O}_3$ powder

Fig. 4.1. x y 가 0.5, $(\text{Pb}_{0.5}, \text{Bi}_{0.5})(\text{Ti}_{0.5}, \text{Fe}_{0.5})\text{O}_3$ X-
 tetragonal, 700 peak
 . , 가
 , , ,
 700 가 .
 900 $c/a=1.135$ tetragonality
 가 Perovskite pattern .
 tetragonality .
 tetragonality 가
 .
 tetragonality
 x y
 . Fig. 4.2 x y 가 가
 x - . x y 가 0.4
 $c/a=1.104 \pm 0.005$, x y 가 0.3
 $c/a=1.090 \pm 0.005$
 tetragonality가 . x y
 tetragonality Table. 4.1. . x y 가 0.2
 0.8 tetragonality가
 tetragonality 가
 .
 Fig. 4.3. x y 가 가 X-

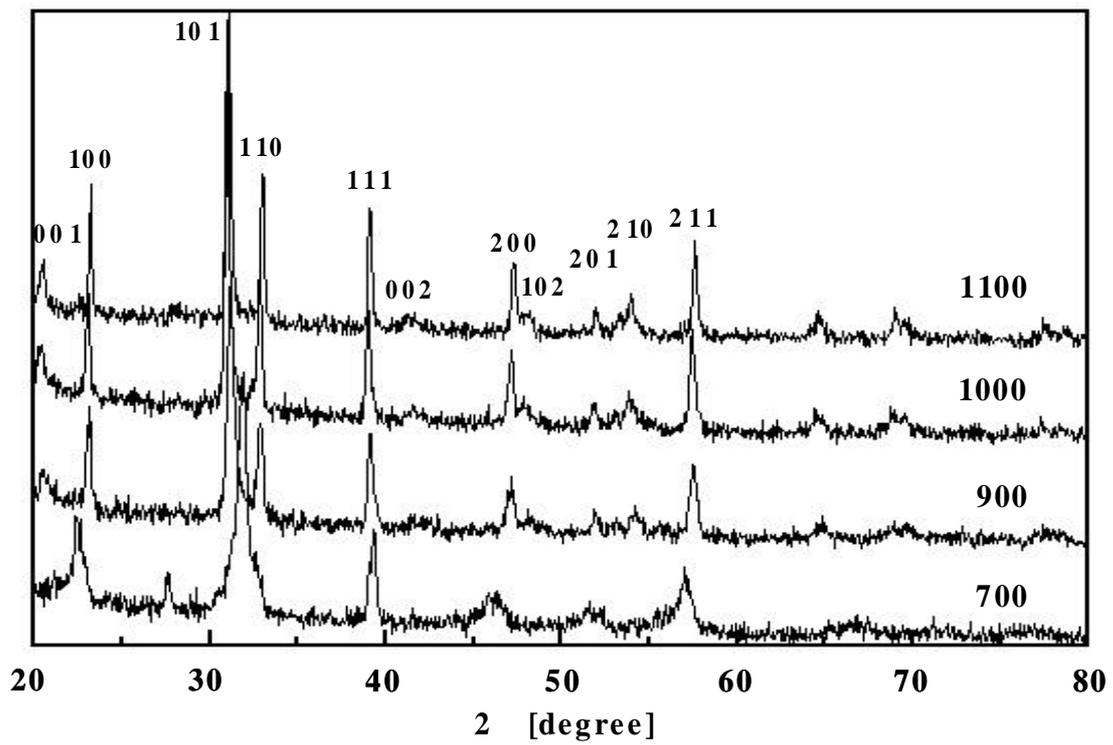


Fig. 4.1. XRD patterns of the powders treated at various temperatures.

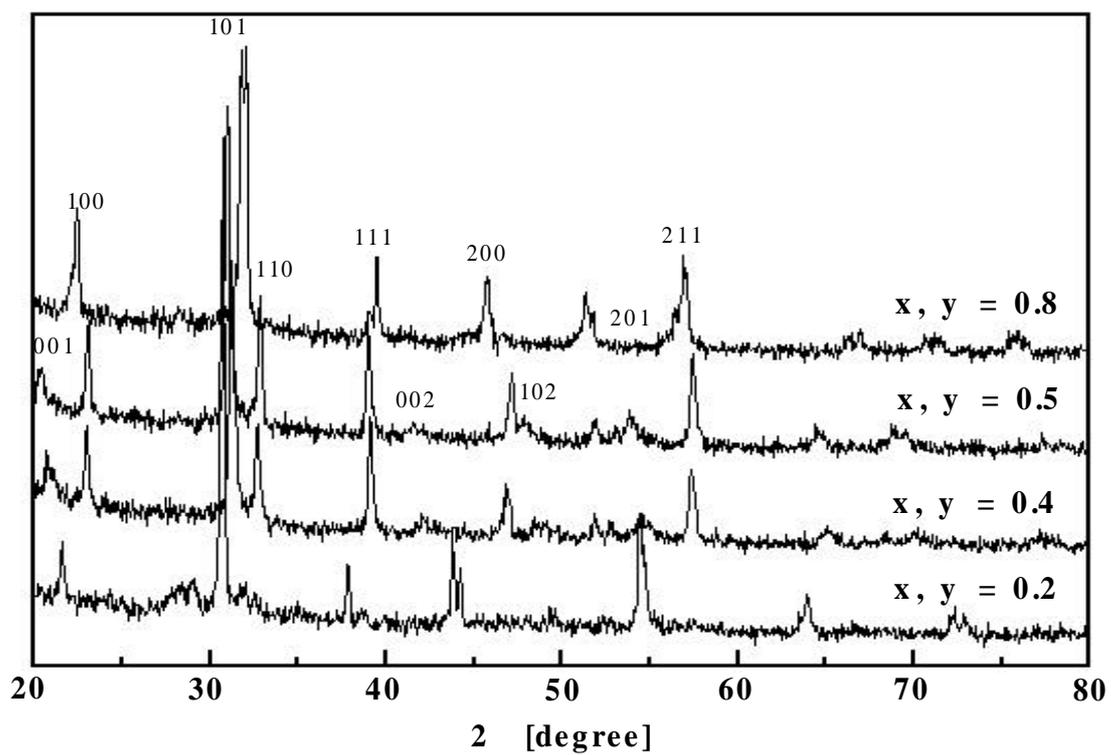


Fig. 4.2. XRD patterns of $(\text{Pb}_{1-x}, \text{Bi}_x)(\text{Ti}_{1-y}, \text{Fe}_y)\text{O}_3$ powder ($x=y$).

Table. 4.1. Tetragonality of each specimen.

Chemical formula	Tetragonality (c/a)
$(\text{Pb}_{0.7}\text{Bi}_{0.3})(\text{Ti}_{0.7}\text{Fe}_{0.3})\text{O}_3$	1.090 ± 0.005
$(\text{Pb}_{0.6}\text{Bi}_{0.4})(\text{Ti}_{0.6}\text{Fe}_{0.4})\text{O}_3$	1.104 ± 0.005
$(\text{Pb}_{0.5}\text{Bi}_{0.5})(\text{Ti}_{0.5}\text{Fe}_{0.5})\text{O}_3$	1.135 ± 0.005

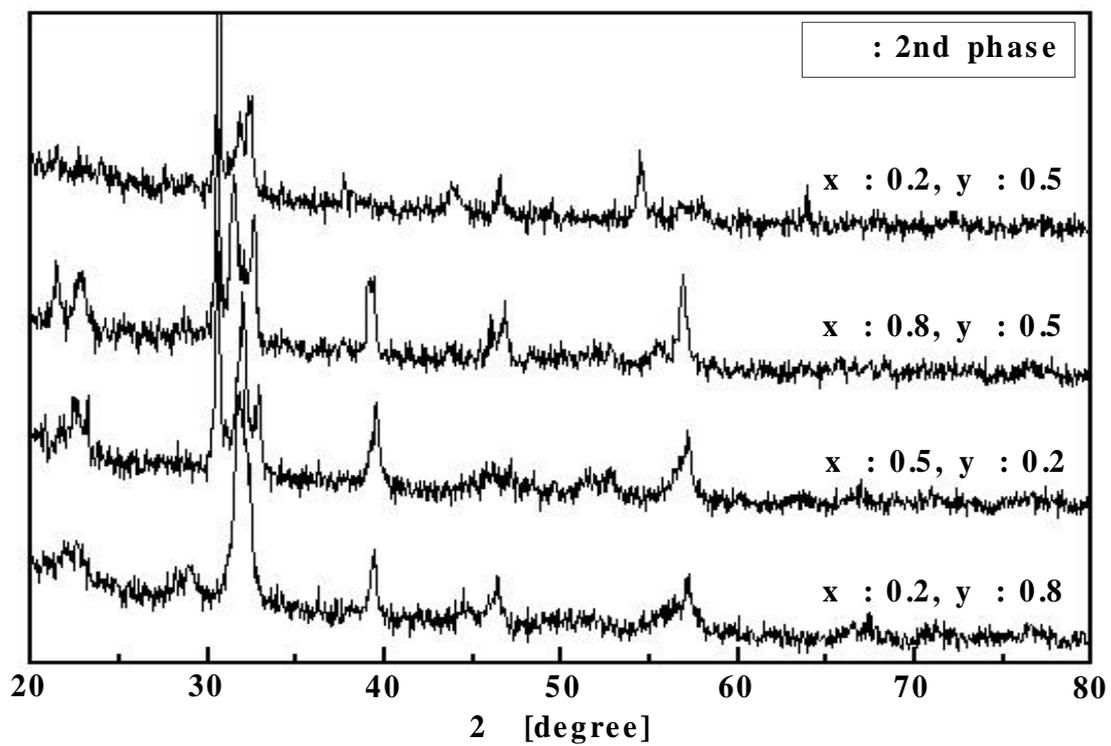


Fig. 4.3. XRD patterns of $(\text{Pb}_{1-x}, \text{Bi}_x)(\text{Ti}_{1-y}, \text{Fe}_y)\text{O}_3$ powder ($x \neq y$).

intensity가 , , 2 =25. 35. 2

2

XRD $(\text{Pb}_{1-x}, \text{Bi}_x)(\text{Ti}_{1-y}, \text{Fe}_y)\text{O}_3$ PbTiO_3

BiFeO_3 , x y가 가

2

tetragonality 가 Perovskite x y가 0.5

가 x y가 가

BiFeO_3 가

tetragonality

tetragonality 가

4.2 $(\text{Pb}_{0.5}, \text{Bi}_{0.5})(\text{Ti}_{0.5}, \text{Fe}_{0.5})\text{O}_3/\text{polymer}$

$(\text{Pb}_{1-x}, \text{Bi}_x)(\text{Ti}_{1-y}, \text{Fe}_y)\text{O}_3/\text{polymer}$ $(\text{Pb}_{1-x}, \text{Bi}_x)(\text{Ti}_{1-y}, \text{Fe}_y)\text{O}_3$

$\text{Fe}_y)\text{O}_3$ 900 1000 . Fig. 4.4 가

X- . (a) (c)가

(b) (d)

$(\text{Pb}_{1-x}, \text{Bi}_x)(\text{Ti}_{1-y}, \text{Fe}_y)\text{O}_3$ Bi-

, Pb 가 가

가

$(\text{Pb}_{1-x}, \text{Bi}_x)(\text{Ti}_{1-y}, \text{Fe}_y)\text{O}_3$ 가 tetragonality 가

$(\text{Pb}_{0.5}, \text{Bi}_{0.5})(\text{Ti}_{0.5}, \text{Fe}_{0.5})\text{O}_3$

polymer 0-3

Fig. 4.5. . $(\text{Pb}_{0.5}, \text{Bi}_{0.5})(\text{Ti}_{0.5}, \text{Fe}_{0.5})\text{O}_3$ (a)

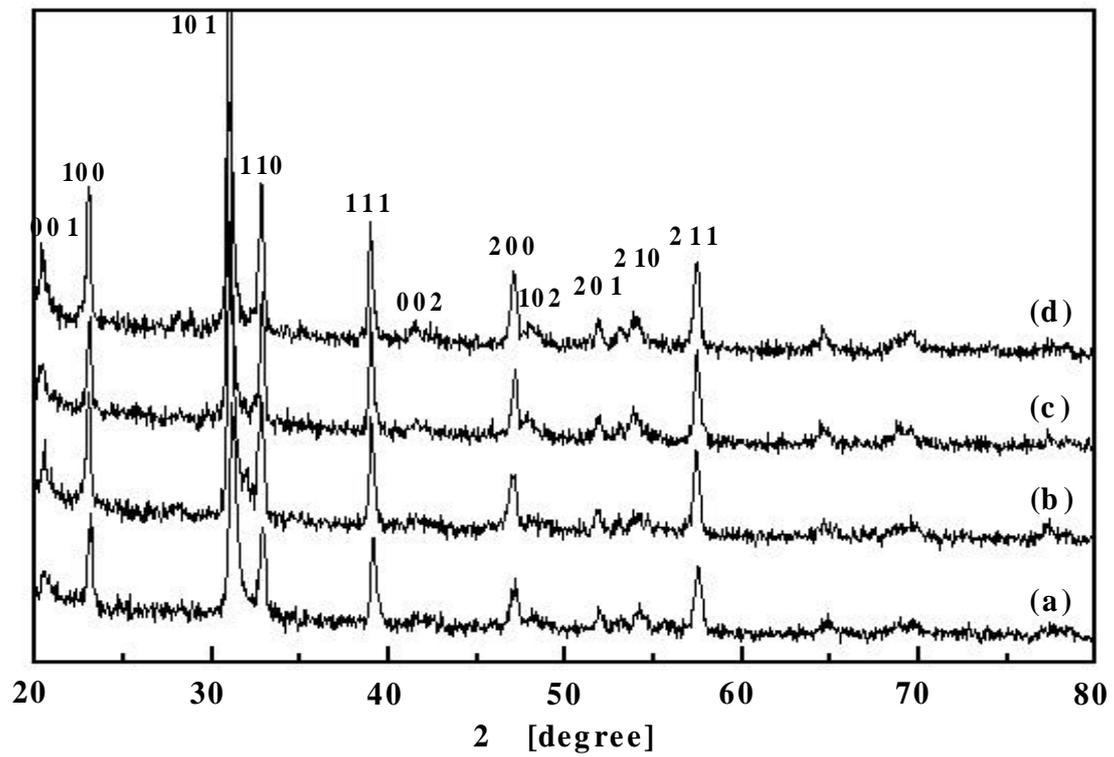


Fig. 4.4. XRD patterns of each heat-treatment conditions.

- (a) 900 °C, Pb-atmosphere (b) 900 °C, air-atmosphere
(c) 1000 °C, Pb-atmosphere (d) 1000 °C, air-atmosphere

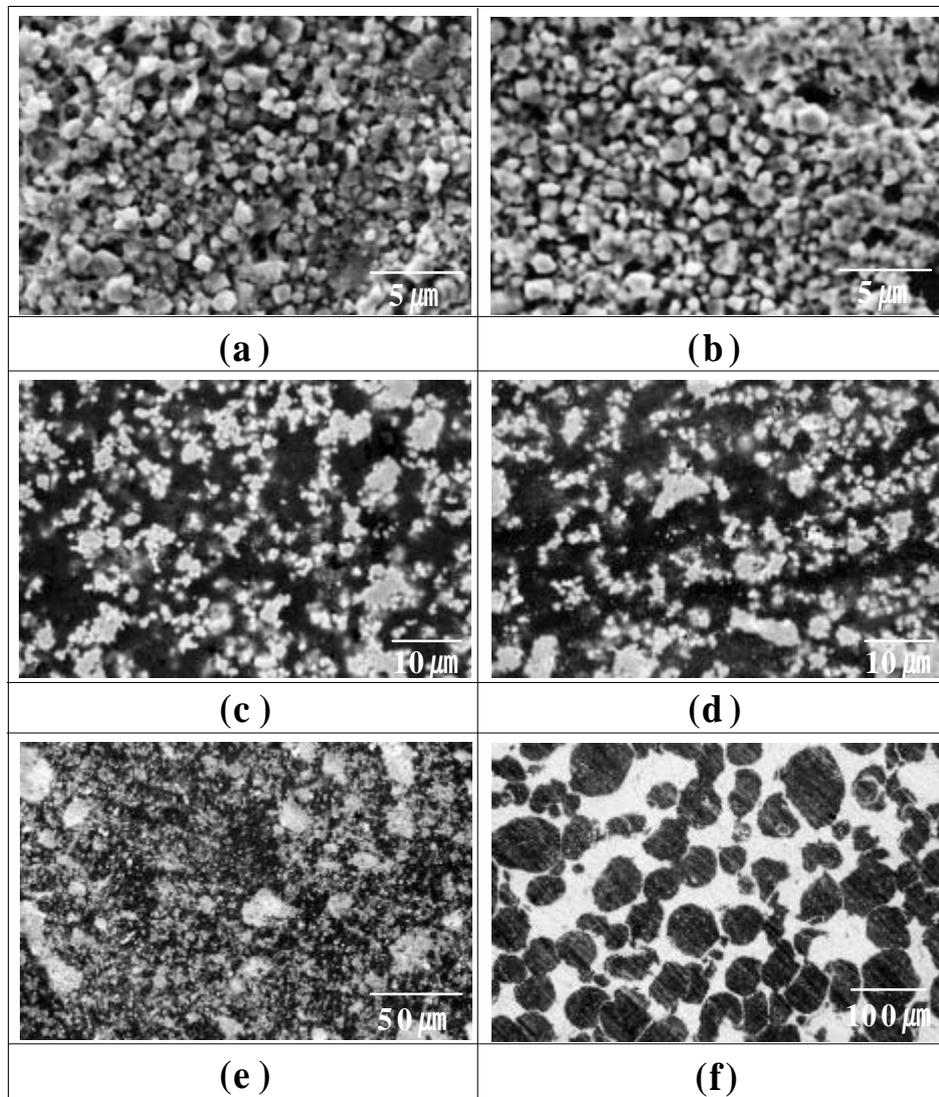


Fig. 4.5. SEM micrographs of (a) ceramic powder sintered at 900 and (b) 1000 , and composite with (c) UP RF1001, (d) KBR1729, (e) Bakelite powder, and (f) Transoptic powder.

(b) 1000 $1\mu\text{m}$ 900
 가 0.7 $1\mu\text{m}$ 가
 $(\text{Pb}_{0.5}, \text{Bi}_{0.5})(\text{Ti}_{0.5}, \text{Fe}_{0.5})\text{O}_3$

(c) (d) 0-3 가
 (f) Transoptic powder
 Transoptic powder
 가 가
 3-0 가 가
 Transoptic powder
 Bakelite powder (e)
 0-3 가
 Bakelite powder 가 가
 30 50vol% 가 LCR Meter

Fig. 4.6.

UP RF1001

Transoptic Powder
 UP RF1001
 가 가 가
 가 40vol%
 가 UP RF1001 20
 40vol% Bakelite Powder
 30 50vol% 가 30vol%
 40vol% Bakelite powder
 UP RF1001 80%

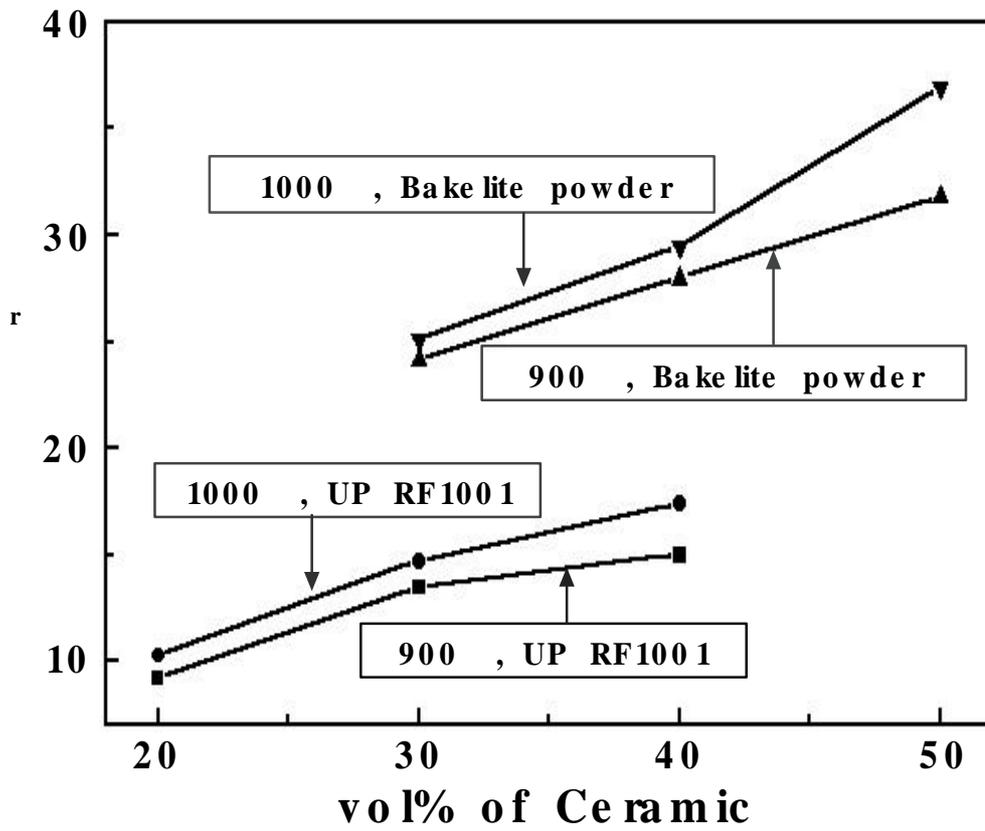


Fig. 4.6. Dielectric properties of each specimens. (1kHz)

가 ,

가 , 900 가 1000

5 15% 가 .

porosity , grain size

shape , distribution

Bakelite Powder 50vol% 가

$r=36.91$ 가 .

Bakelite powder RT 66A

hysteresis loop Fig. 4.7. . (a) 900 , (b) 1000

hysteresis loop

$(Pb_{0.5}, Bi_{0.5})(Ti_{0.5}, Fe_{0.5})O_3$ 가

900

1000

Fig. 4.8. 900 $(Pb_{0.5}, Bi_{0.5})(Ti_{0.5}, Fe_{0.5})O_3$ 50vol%

가 가 Graph .

가 가 6kV/mm

$(Pb_{0.5}, Bi_{0.5})(Ti_{0.5}, Fe_{0.5})O_3$

tetragonality 가

domain

가 . $(Pb_{0.5},$

$Bi_{0.5})(Ti_{0.5}, Fe_{0.5})O_3$ poling

6kV/mm

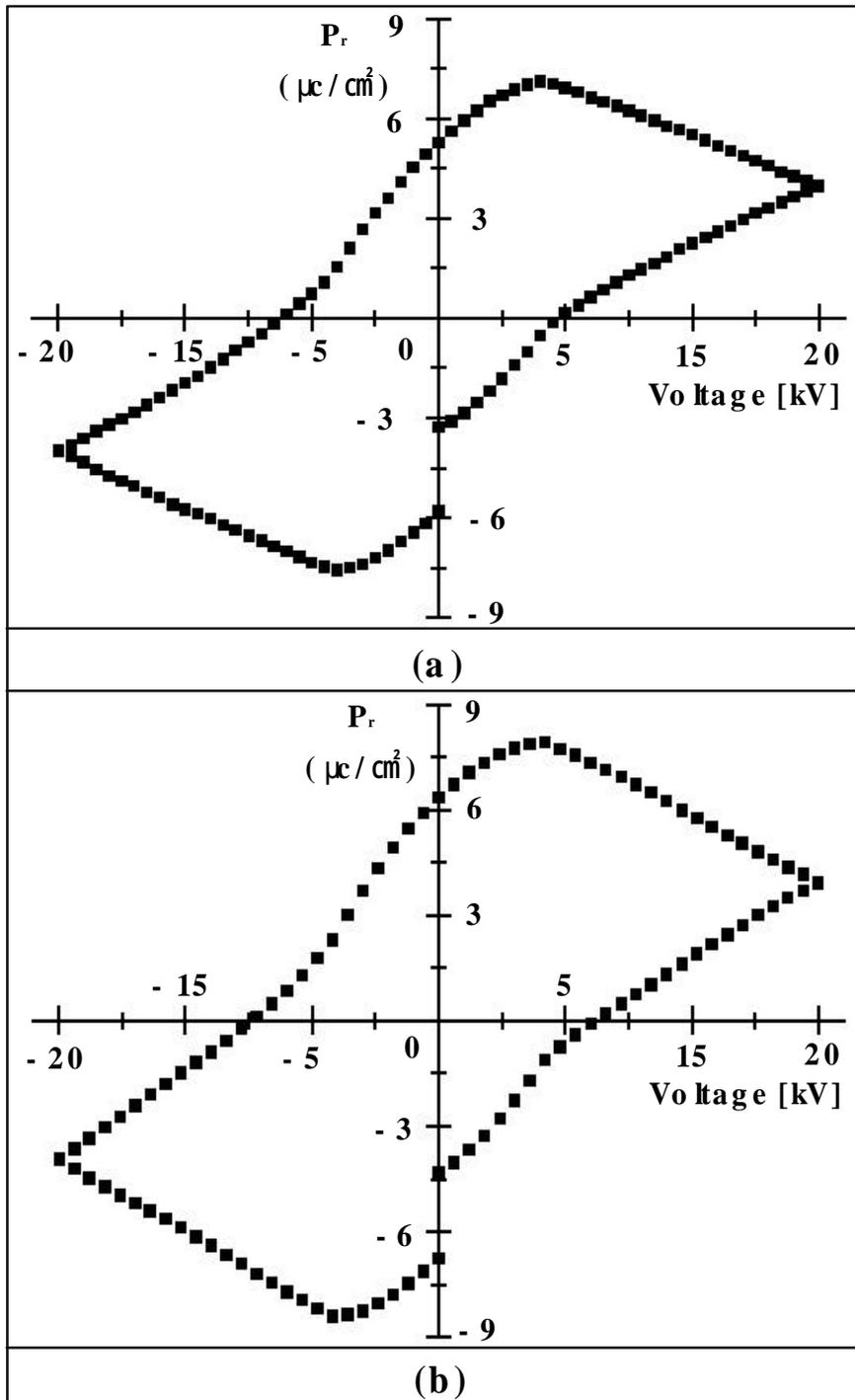


Fig. 4.7. Hysteresis loop of specimens: composite with Bakelite powder and $(\text{Pb}_{0.5}\text{Bi}_{0.5})(\text{Ti}_{0.5}\text{Fe}_{0.5})\text{O}_3$ calcined at (a) 900 , and (b) 1000 .

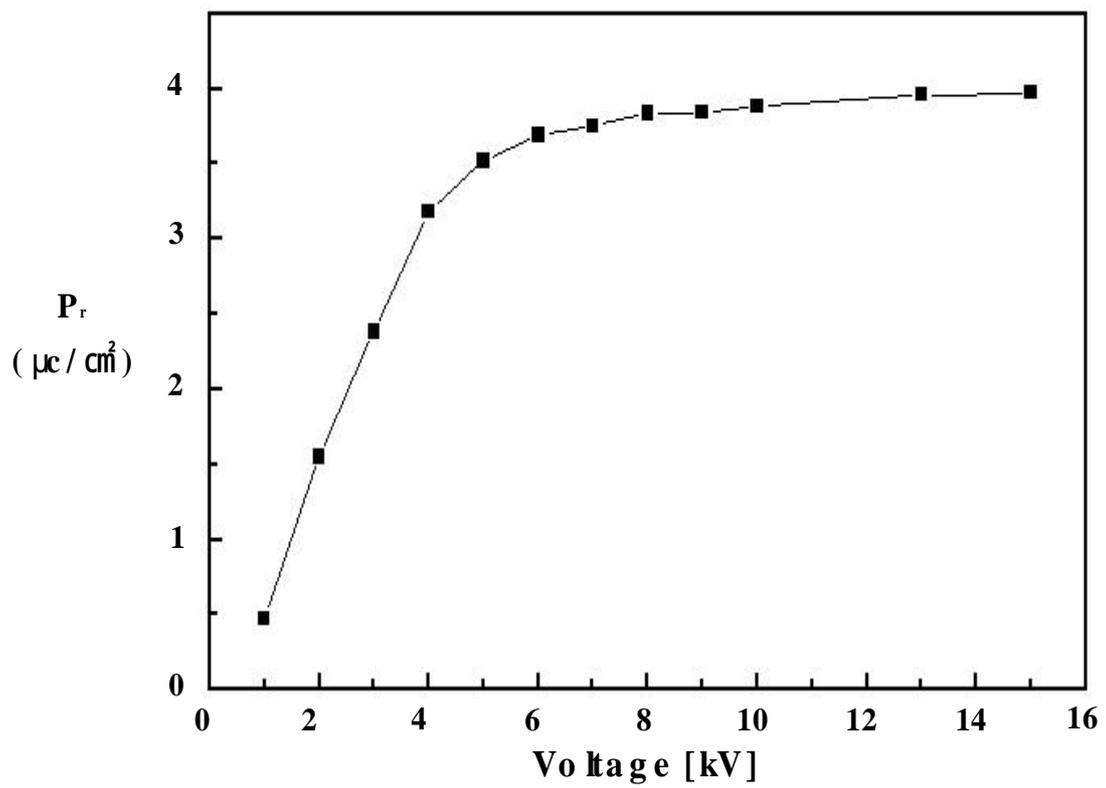


Fig. 4.8. Remanent polarizations of the 50vol% of $(\text{Pb}_{0.5}\text{Bi}_{0.5})(\text{Ti}_{10.5}\text{Fe}_{0.5})\text{O}_3$ calcined at 900 composite with each voltage.

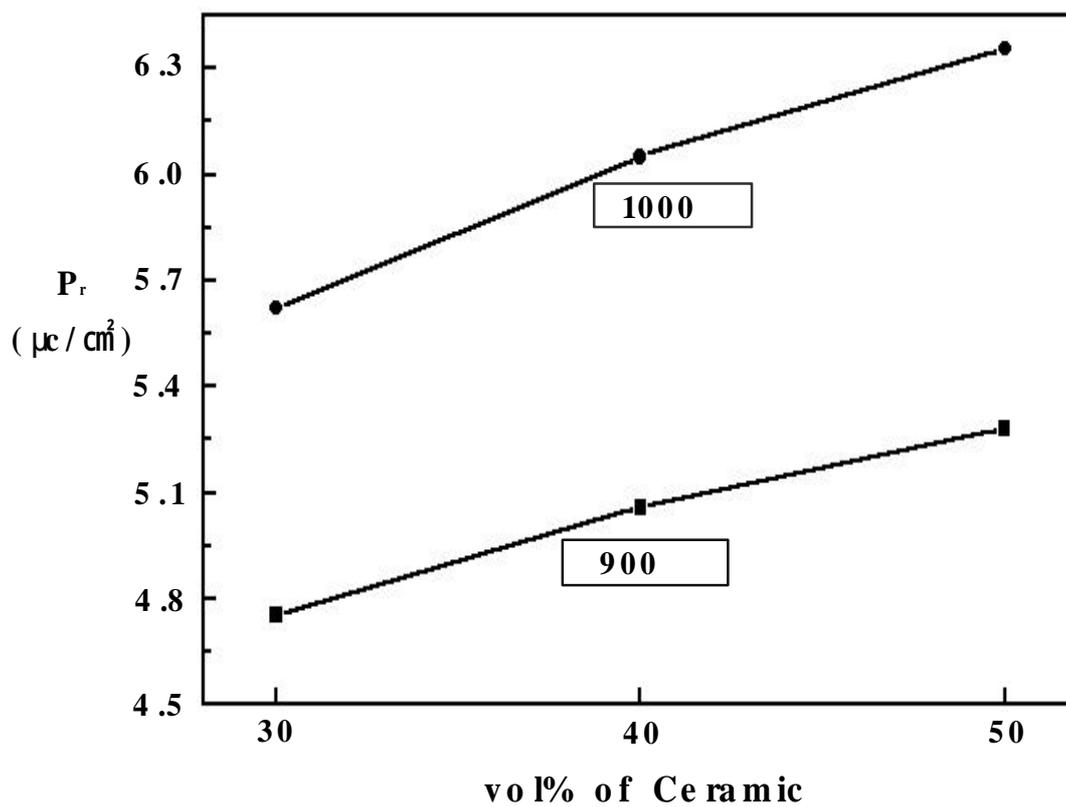
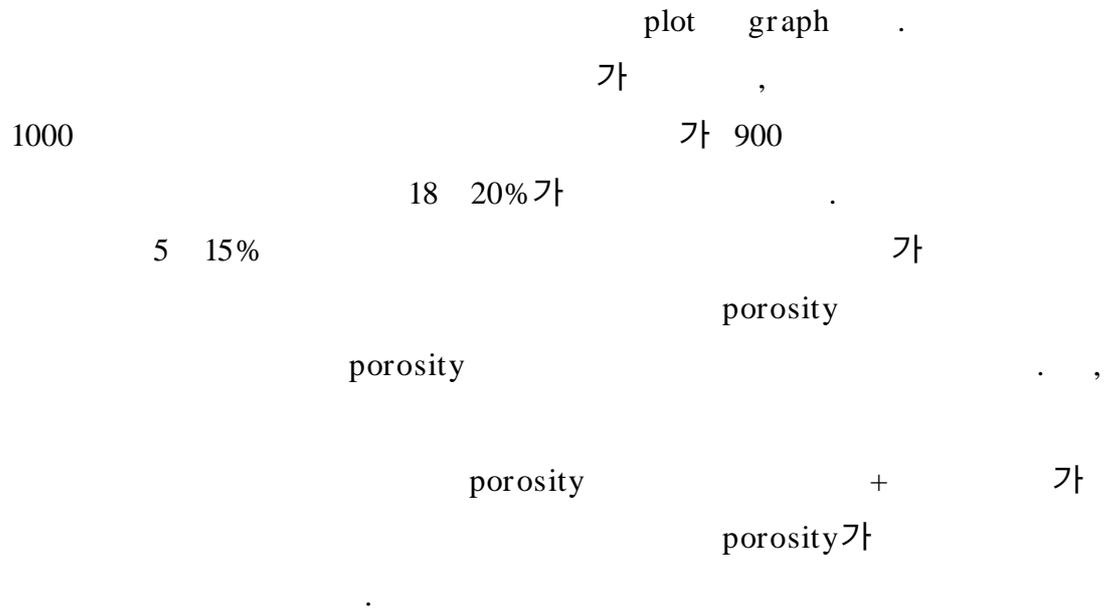


Fig. 4.9. Remanent polarizations of the composites with Bakelite powder with each vol% of $(\text{Pb}_{0.5}\text{Bi}_{0.5})(\text{Ti}_{10.5}\text{Fe}_{0.5})\text{O}_3$.

Fig. 4.9. Bakelite powder



5.

PbO, Bi₂O₃, TiO₂, Fe₂O₃ (Pb_{1-x},
 Bi_x)(Ti_{1-y}, Fe_y)O₃ , polymer 0-3

1. PbO, Bi₂O₃, TiO₂, Fe₂O₃ (Pb_{1-x},
 Bi_x)(Ti_{1-y}, Fe_y)O₃ .

2. , (Pb_{1-x}, Bi_x)(Ti_{1-y}, Fe_y)O₃ PbTiO₃
 BiFeO₃ .

3. x=y가 2 .

4. x, y = 0.5 가 tetragonality (c/a=1.135 ± 0.005)
 BiFeO₃ 가 tetragonality
 tetragonality가 .

5. tetragonality . (Pb_{0.5},
 Bi_{0.5})(Ti_{0.5}, Fe_{0.5})O₃ 0-3 .

6. 가 가
 , 1000 50vol% 가 ε_r = 36.91 가

7. 1000
 가 900 5 15% 가
 가 .

8. RT 66A hysteresis loop , 6kV/mm
가 , 1000 50vol% 가
Pr=6.355 $\mu C/cm^2$ 가 .

9. 1000
가 900 18
20% 가 가
가 porosity
.

- 1) , , ' . - ', , (1991).
- 2) G. Busch, 'Early History of Ferroelectric', *Ferroelectric*, **74**, 267, (1987).
- 3) W. Kanzig, 'History of Ferroelectricity 1938- 1955', *Ferroelectric*, V74, 285, (1987).
- 4) T. Kitayama, 'Flexible Piezoelectric Materials', *Ceramics*, **14**(3), 209, (1979).
- 5) Koss LL, Simon GP, Law HH, 'Mechanisms in Damping of Mechanical Vibration by Piezoelectric Ceramic Polymer Composite-Materials', *Journal of Materials Science*, **30**(10), 2648 2655, (1995).
- 6) Yang TCK, Viswanath DS, In Situ, 'Measurement of Emissivities of Ceramic-Polymer Composite-Materials', *Journal of the American Ceramic Society*, **80**(1), 157 164, (1997).
- 7) Janas-VF, McNulty-TF, Walker-FR, Schaeffer-RP, Safari-A, 'Processing of 1-3 Piezoelectric Ceramic/Polymer Composites', *Journal of the American Ceramic Society*, **78**(9), 2425 2430, (1995).
- 8) McNulty TF, Janas VF, Safari A, Loh RL, Cass RB, 'Novel Processing of 1-3-Piezoelectric Ceramic/Polymer Composites for Transducer Applications', *Journal of the American Ceramic Society*, **78**(11), 2913 2916, (1995).
- 9) Tan-LS, Mchugh-AJ, 'The Role of Particle-Size and Polymer Molecular-Weight in the Formation and Properties of an Organo-Ceramic Composite', *Journal of Materials Science*, **31**(14), 3701 3706 (1996).
- 10) Takenaka T, Yamada M, Okuda T, 'Development of new piezoelectric ceramics with bismuth perovskites', ISAF '94. Processing of the Ninth IEEE International Symposium on Applications of Ferroelectrics (Cat. No.94CH3416-5). (1994).

- 11) Han K H, Riman R E, Safari A, 'Lead Bismuth titanium iron oxide $[(\text{Pb}_{0.5}\text{Bi}_{0.5})(\text{Ti}_{0.5}\text{Fe}_{0.5})\text{O}_3]$ powder prepared by chemically precipitated method for O_3 ceramic/polymer composites'. *Ceram. Trans.* **8**(Ceram. Dielectr.: Compos., Process. Prop.), 227-232, (1993).
- 12) Takenaka Tadashi, Yamada Masatoshi, 'Ferroelectric properties of bismuth lead nickel titanate $(\text{Bi}_{1/2}\text{Pb}_{1/2})(\text{Ni}_{1/4}\text{Ti}_{1/4})\text{O}_3$ for new piezoelectric ceramics', *Jpn. J. Appl. Phys. 2, Lett.* **32**(7A), L928-L931, (1993).
- 13) Ozeki Hirofumi, Hishida Kunihiro, Ohya Kanji, Banno Hisao, 'Manganese dioxide-added lead bismuth neodymium titanate $[(\text{Pb}, \text{Bi}, \text{Nd})\text{TiO}_3]$ ceramics and their application to cylinder pressure sensors', *Sens. Mater.* **2**(1), 27-38, (1990).
- 14) Han KH, Riman RE, Safari A, 'Preparation of lead bismuth titanium iron oxide $[(\text{Pb}_{0.5}\text{Bi}_{0.5})(\text{Ti}_{0.5}\text{Fe}_{0.5})\text{O}_3]$ ceramic powder from metal organic precursors for O_3 ceramic/polymer composites', *Ultrastruct. Process. Adv. Mater.*, [Proc. Int. Conf. Ultrastruct. Process. Ceram., Glasses Compos.], 4th. 377-384, (1993).
- 15) Yoneda Atsuhiko, Takenaka Tadashi, Sakata Koichiro, 'Temperature dependence of piezoelectric constants of lithium bismuth $(\text{Li}_{0.5}\text{Bi}_{0.5})$ -modified PZT (lead zirconate-lead titanate) ceramics in the vicinity of the morphotropic phase boundary', *Nippon Seramikkusu Kyokai Gakujutsu Ronbunshi* **98**(8), 890-894. Japan, (1990).
- 16) Reaney, Ian M, Damjanovic, Dragan, 'Crystal structure and domain-wall contributions to the piezoelectric properties of strontium bismuth titanate ceramics', *J. Appl. Phys.* **80**(7), 4223-4225, (1996).
- 17) Li Z, Forster CM, Dai XH, Xu Xz, Chan SK, Lam DJ, 'Piezoelectrically-induced switching of $90(+)$ domains in tetragonal bismuth titanate and lead titanate investigated by micro-Raman spectroscopy', *J. Appl. Phys.* **71**(9), 4481-4486, (1992).

18) Janas-VF, Safari-A, Overview of Fine-Scale 'Piezoelectric Ceramic/Polymer Composite Processing', Journal of the American Ceramic Society, **78**(11), 2945-2955, (1995).

19) Chu SZ, Sakairi M, Takahashi H, Simamura K, Abe K, 'Laser-assisted electroless Ni-P deposition at selected areas on Al (-Mg, Si, Cu) alloys', Journal of the Electrochemical Society, **147**(6), (2000)